*METALS AND MATERIALS International, Vol. 8, No. 4 (2002), pp. 375~379*

# Cyclic Oxidation Behavior of $Ni_3Al$-7.8%Cr-1.3%Zr-0.8%Mo-0.025%B between 900 and 1100°C

**Gi-Young Kim and Dong-Bok Lee**

Center for Advanced Plasma Surface Engineering, Sungkyunkwan University
300 Cheoncheon-dong, Jangan-gu, Suwon 440-746, Korea

A $Ni_3Al$-based alloy, the composition of which was Ni-16.0%Al-7.8%Cr-1.3%Zr-0.8%Mo-0.025%B, was cyclically oxidized in the temperature range of 900 to 1100°C in air for up to 500 hr. The alloy displayed good cyclic oxidation resistance up to 1000°C, with little scale spallation. It, however, lost cyclic oxidation resistance during oxidation at 1100°C after about 200 hr, displaying large weight losses due to serious scale spallation. NiO, $\alpha$-$Al_2O_3$, $NiAl_2O_4$ and $ZrO_2$ were formed. The oxide scales consisted primarily of an outer Ni-rich layer which was prone to spallation, and (Al, Cr, Zr, Mo, Ni)-containing internal oxides which were adherent due mainly to the formation of ($Al_2O_3$, $ZrO_2$)-containing oxides that keyed the oxide scale to the matrix alloy.

**Keywords :** $Ni_3Al$, intermetallics, cyclic oxidation, chromium, zirconium, molybdenum

## 1. INTRODUCTION

Nickel aluminides based on $Ni_3Al$ have received considerable attention for high temperature structural applications due to their high stiffness and strength retention at elevated temperatures, combined with low density and good oxidation resistance. The additions of Cr and Mo that were soluble up to several percent in $Ni_3Al$, together with small amounts of Zr and B that were segregated at the grain boundaries, improved strength and tensile ductility by solid-solution hardening and by enhancing grain-boundary cohesive strength, respectively [1]. Concerning oxidation, the 2.9%Cr addition to $Ni_3Al$ [2] slightly increased the isothermal oxidation resistance by the gettering effect of Cr, the oxide of which was intermediate in stability between NiO and $Al_2O_3$, which formed during oxidation. The 0.1%B addition to $Ni_3Al$ enhanced the growth of an $Al_2O_3$ layer, however it did not improve the scale adherence nor the formation of voids on the matrix surface [3]. The 2.2%Zr addition to $Ni_3Al$-0.1%B increased the oxidation rate greatly, though the scale adherence was increased [3]. These effects of Cr, B and Zr were validated by Klöwer *et al*. [4] and Chuang *et al*. [5,6]. The scales that formed on $Ni_3Al$-(0.3~2%)Zr [5], $Ni_3Al$-0.1%B-2.2%Zr [3], and $Ni_3Al$-8%Cr-1%Zr-0.2%B [6] consisted of NiO, $ZrO_2$, $\alpha$-$Al_2O_3$ and $NiAl_2O_4$. The previous oxidation studies [4-6] were focused on the isothermal oxidation behavior of $Ni_3Al$ alloys having Cr and/or Zr and/or B; however, the oxidation behavior of the present alloy including cyclic oxidation has not yet been adequately studied. This paper aims to investigate the cyclic oxidation behavior of the $Ni_3Al$-Cr-Zr-Mo-B alloy between 900 and 1100°C in air.

## 2. EXPERMENTAL PROCEDURE

The chemical composition of the prepared alloy was 74.028% Ni-16.004%Al-7.844%Cr-1.263%Zr-0.836%Mo-0.025%B (at.%). The alloy that was centrifugally cast into a pipe with an outside diameter of 36 cm was cut into coupons of $4\times6\times15$ $mm^3$, polished on 1000 grit paper, and ultrasonically cleaned in acetone and alcohol for oxidation tests.

Cyclic oxidation tests were performed at 900, 1000 and 1100°C in atmospheric air using a tube furnace. The test cycles involved exposing the specimens for 1 hr, cooling quickly to room temperature, and returning them to the furnace. The specimens during cyclic oxidation were given a total exposure of 500 hr (500 cycles). The heating rate was 350°C/min, and the cooling rate was 150°C/min. The weight changes during tests were measured intermittently using a microbalance with an accuracy of $10^{-4}$g, excluding spontaneously spalled oxide scales. The oxidized specimens were inspected by an X-ray diffractometer (XRD), and a scanning electron microscope (SEM) equipped with an energy dispersive spectrometer (EDS).

## 3. RESULTS AND DISCUSSION

Fig. 1 shows the microstructure of the prepared $Ni_3Al$-Cr-Zr-Mo-B alloy. A dendrite structure is seen. The XRD tests

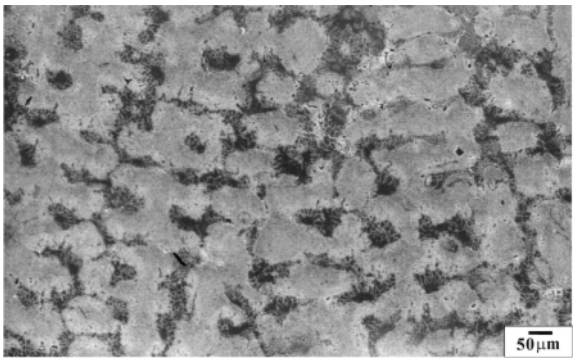


**Fig. 1.** SEM micrograph of the prepared $Ni_3Al$-Cr-Zr-Mo-B alloy. Etched with (50 ml nitric acid+50 ml distilled water).

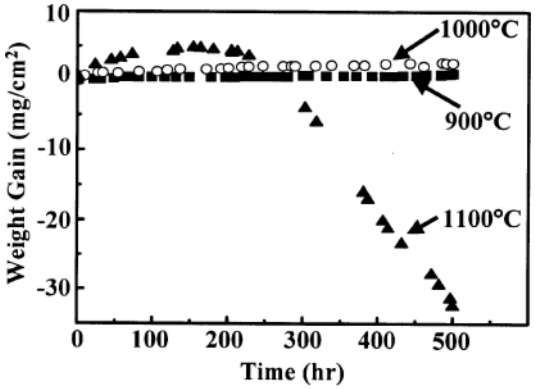


**Fig. 2.** Cyclic oxidation curves of $Ni_3Al$-Cr-Zr-Mo-B alloy at 900, 1000 and 1100°C in air.

revealed that the matrix consisted primarily of γ'-$Ni_3Al$.

The results of cyclic oxidation tests on the prepared alloy at 900, 1000 and 1100°C are displayed in Fig. 2. The alloy exhibited an excellent cyclic oxidation resistance up to 1000°C, with little oxide spallation. It, however, suffered from continuous weight losses owing to the ensuing scale-spallation, after initial oxidation of about 200 hr at 1100°C. Clearly, the accumulated large growth stress, together with thermal stress generated during thermal cyclings, urged the oxide scale to spall severely as the scale thickened.

Fig. 3 shows the XRD results of the cyclically oxidized alloys. The X-ray diffraction patterns at 900, 1000 and 1100°C reveals patterns of [$Ni_3Al$(vs), NiO(s), α-$Al_2O_3$(w)], [$Ni_3Al$(vs), NiO(s), α-$Al_2O_3$(m), $NiAl_2O_4$(m), monoclinic-$ZrO_2$(vw), tetragonal-$ZrO_2$(w)], and [$Ni_3Al$(s), NiO(vs), α-$Al_2O_3$(m), $NiAl_2O_4$(w), monoclinic-$ZrO_2$(vw), tetragonal-$ZrO_2$(vw)], respectively. The observed, strong $Ni_3Al$ intensity was due to thin scale formation and/or exposure of a fresh surface owing to scale spallation. The NiO always displayed the strongest patterns among the oxide formed. The ability to form the alumina, which partially reacted with NiO to form the $NiAl_2O_4$ spinel, increased with an increase in oxidation temperature [3,5]. A very small amount of $ZrO_2$ coexisted in the form of low-temperature monoclinic and high-temperature tetragonal structures. This is different from the XRD results of isothermally oxidized $Ni_3Al$-(0.3-2%)Zr(-8%Cr-0.2%B) alloys, where monoclinic-$ZrO_2$ and tetragonal-$ZrO_2$ were reported to form below and above the transformation temperature of 1050°C, respectively [5,6]. On the other hand, our previous study on both isothermally and cyclically grown oxide scales that formed on a $Ni_3Al$-8%Cr-1%Zr-0.1%B alloy under similar oxidation conditions showed the coexistence of both monoclinic- and tetragonal-$ZrO_2$ [7]. Though polymorphic forms of existing $ZrO_2$ reported by Chuang *et al.* [5,6] did not match with our results, the other oxidation products of NiO, α-$Al_2O_3$ and $NiAl_2O_4$ were unanimously reported to exist in all the Zr-containing alloys [3-6]. Interestingly, no Cr-oxides were found, although the Cr content was higher than Zr in the matrix alloy [6]. This strongly indicates that Cr-oxides were present as dissolved ions by forming a solid solution with the X-ray detected oxide phases. The oxides of Mo and B were also undetectable probably due to their small amount or dissolution in the oxide phases.

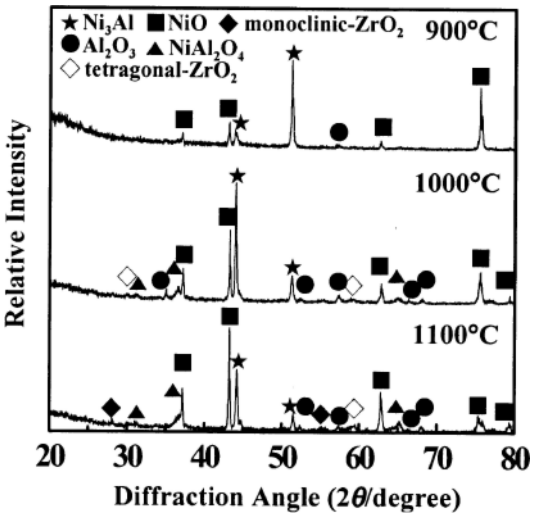


**Fig. 3.** XRD patterns of the scales formed after cyclic oxidation for 500 hr at 900, 1000 and 1100°C in air.

Fig. 4 depicts the SEM top view and cross-sectional image of the oxide scale formed after cyclic oxidation at 900°C for 500 hr. Despite cyclic oxidation, there was virtually no indication of any scale spallation. Fine, round oxide grains were formed over the polished alloy surface (Fig. 4(a)). Beneath the polished alloy surface, internal oxidation occurred along the matrix grain boundaries (Fig. 4(b)) [3-6]. Apparently, the outer oxide grains were formed by the outward diffusion of cations, while internal oxide stringers were formed mainly by the inward transport of oxygen. The location where internal oxidation occurred seemed to depend on specific composition and/or orientation of each matrix grain.

Fig. 5 shows the SEM top view, the cross-sectional image

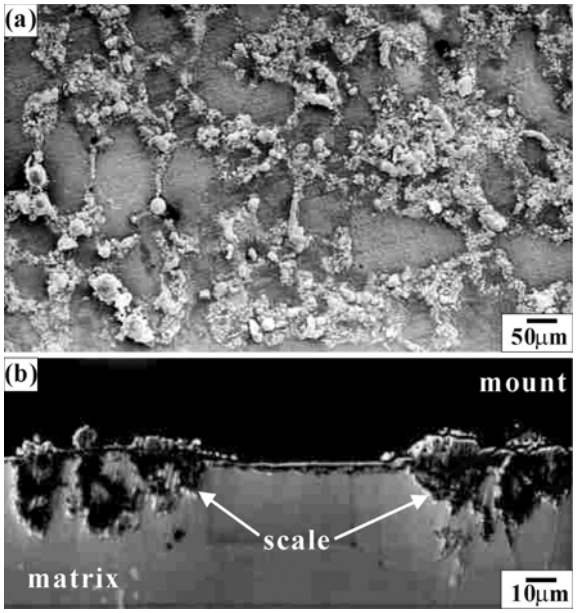


**Fig. 4.** SEM images of the oxide scale formed after cyclic oxidation at 900°C for 500 hr: (a) top view; and (b) cross-sectional image.

and the corresponding EDS elemental mappings of the oxide scale formed after cyclic oxidation at 1000°C for 500 hr. Since boron that was added at 0.025% was unidentifiable even when EPMA was used, the boron mapping was omitted. The morphology at 1000°C was basically similar to that at 900°C. The noticeable differences of Fig. 5 from Fig. 4 were: (1) the oxide grains that formed over the polished alloy surface were more widespread, because of increased extent of oxidation (Fig. 5(a)), and (2) internal oxide stringers were more widespread and penetrated deeper into the matrix alloy (Fig. 5(b)). The elemental mappings shown in Fig. 5(c) indicate that the depletion of Ni around the scale-matrix interface are owing to the consumption of Ni to form the oxide scale. Aluminum was strongly segregated at the lower part of the oxide scale as internal oxide stringers. Chromium also tended to segregate beneath the outer, Ni-rich oxide scale, but to a less extent. Zirconium behaved like Cr to segregate at the lower part of the oxide scale. Particularly, Zr, which was segregated along the matrix grain boundaries prior to oxidation, was also oxidized along the grain boundaries which were fast diffusion paths for the inwardly penetrating oxygen ions [3]. Nickel was seen to be depleted at the grain boundaries. Though unclear due mainly to its small content in the alloy, no segregation of Mo appeared to occur. The uneven penetration of internal oxide stringers enriched with $Al_2O_3$ and $ZrO_2$ can improve the scale adherence by the so-called keying mechanism [3]. Though the scale adherence was generally good at 1000°C as was observed at 900°C, the oxide scale formed at 1000°C was somewhat susceptible to scale spallation, as could be envisaged from some pores or

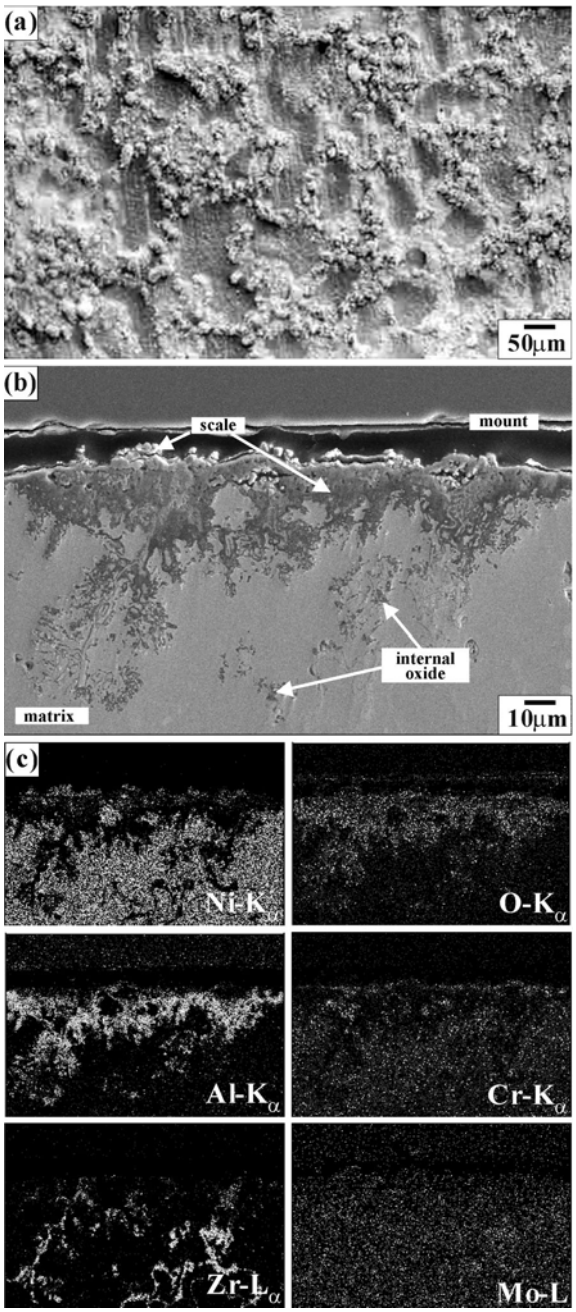


**Fig. 5.** SEM/EDS results of the oxide scale formed after cyclic oxidation at 1000°C for 500 hr: (a) top view; (b) cross-sectional image; and (c) elemental mappings of Ni, O, Al, Cr, Zr and Mo for (b).

cracks inside the oxide scale (Fig. 5(b)). Particularly, the outer, NiO-enriched oxides were found to spall, whereas the internal oxide stringers were quite adherent.

Fig. 6 displays the SEM top view and the corresponding elemental mappings of the oxide scale formed after cyclic oxidation at 1100°C for 90 hr. Ni was more strongly enriched at the outer scale than the inner, adherent scale where Al, Cr, and Zr were segregated. The adherent scale (outer scale)

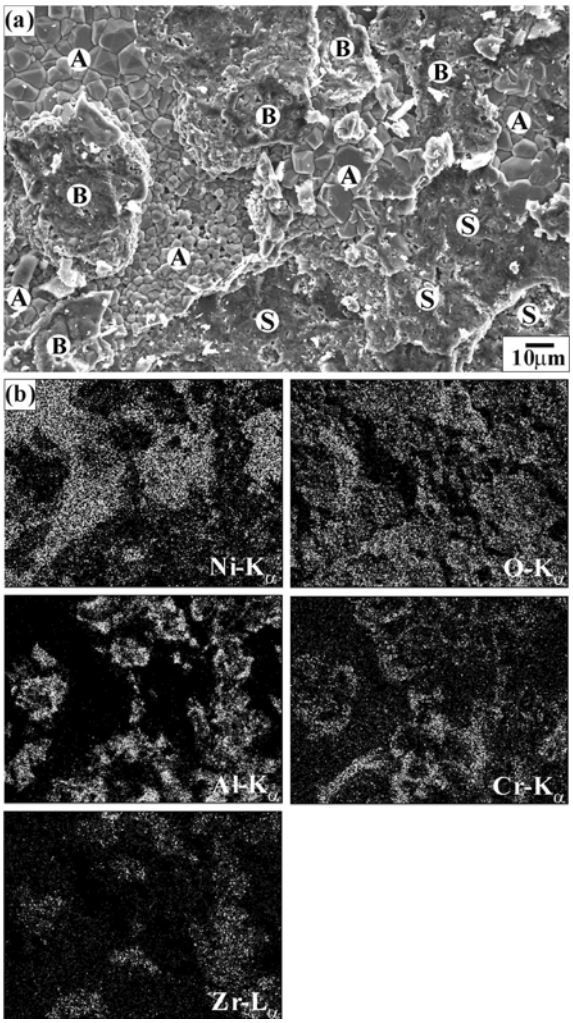


**Fig. 6.** SEM top view of the scale formed after cyclic oxidation at 1100°C for 90 hr: (a) image; and (b) mapping of Ni, O, Al, Cr and Zr. 'A' means an adherent scale, and 'S' means the oxide-spalled region. 'B' is the back-side of the detached scale.

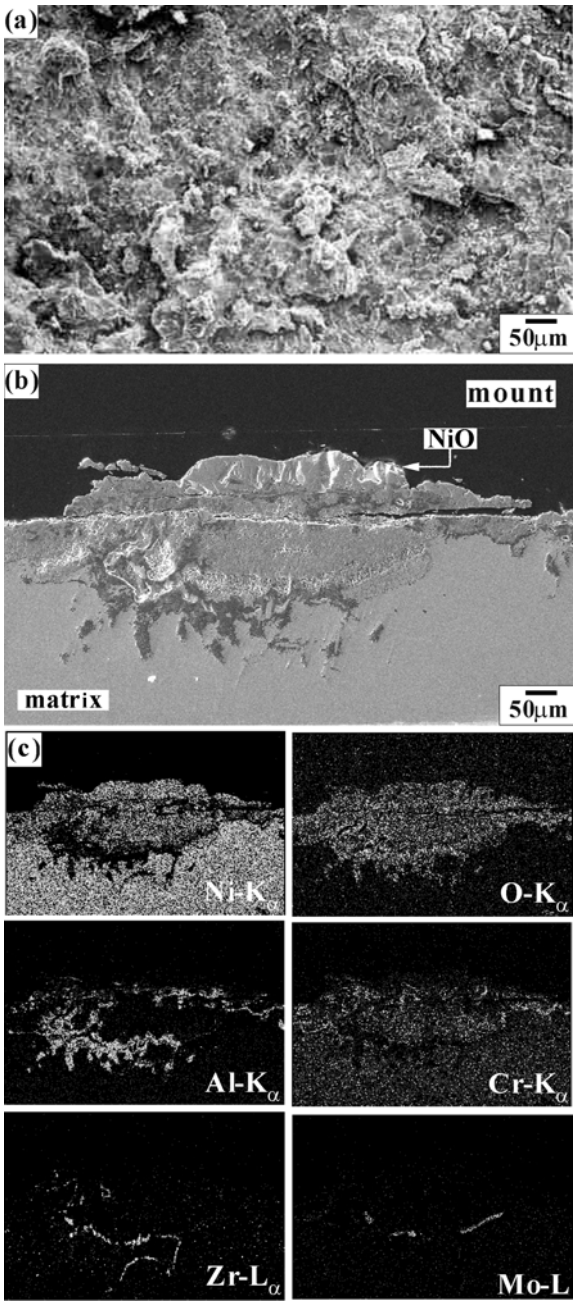


**Fig. 7.** SEM/EDS results of the oxide scale formed after cyclic oxidation at 1100°C for 500 hr: (a) top view; (b) cross-sectional image; and (c) elemental mappings of Ni, O, Al, Cr, Zr and Mo for (b).

consisted primarily of coarse, round NiO grains. Beneath the detached scale, fine, round oxide grains that consisted mainly of $NiAl_2O_4$ and $ZrO_2$ existed.

Fig. 7 shows the top view, the cross-sectional image and the corresponding elemental mappings of the oxide scale formed after cyclic oxidation at 1100°C for 500 hr. The oxide surface was quite rough due to extensive scale spallation (Fig. 7(a)). Most of the outer, NiO-rich oxide layer spalled, and the adherent scale such as that shown in Fig. 7(b) was scarce. The EDS mappings shown in Fig. 7(c) imply that the outermost scale was essentially pure NiO, beneath which mixed oxides of Ni, Al, Cr and Zr existed. Dark areas below the NiO-rich oxide layer in Fig. 7(b) were Al-rich oxides (mostly a-$Al_2O_3$). The active elements of Al and Zr preferentially existed around the scale-matrix interface of which adherence was good. A rather uniform distribution of Cr beneath the NiO layer as well as some segregation of Mo at the lower part of the oxide stringers were recognizable. The above results indicated that Ni, being the major matrix element, constituted the whole oxide scale. Oxides of Al and Zr tended to form internally without forming a continuous, protective oxide layer. Chromium, which was more active than Ni and Mo, but nobler than Al and Zr [8], oxidized preferen-

tially beneath the outermost NiO layer. The oxidation of Mo was less distinct due mainly to its low content or activity in the matrix.

## 4. CONCLUSIONS

The cyclic oxidation behavior of the $Ni_3Al$-Cr-Zr-Mo-B alloy was studied between 900 and 1100°C. Although the scales formed were generally adherent, serious scale spallation occurred after oxidation at 1100°C for about 200 hr. Spallation occurred mainly at the outer part of the oxide scale enriched with NiO, beneath which $Al_2O_3$, $NiAl_2O_4$ and $ZrO_2$ were presented primarily as internal oxides. The bottom part of internal oxides that consisted primarily of $Al_2O_3$ and $ZrO_2$ keyed the oxide scale. Oxides of Cr were present as dissolved ions primarily beneath the outer, NiO-rich scale.

## ACKNOWLEDGMENTS

This study was supported by the Center for Advanced Plasma Surface Technology at Sungkyunkwan University and the BK 21 program of the Ministry of Education, Korea.

## REFERENCES

1. C. T. Liu and K. S. Kumar, *JOM* **45**, May, 38 (1993).
2. S. C. Choi, H. J. Cho, and D. B. Lee, *Oxid. Met.* **46**, 109 (1996).
3. S. Taniguchi and T. Shibata, *Oxidation of High-Temperature Intermetallics* (eds., T. Grobstein and J. Doychak), p. 17, TMS, Warrendale, PA (1988).
4. J. Klöwer, U. Brill, and U. Heubner, *Inermetallics* **7**, 1183 (1999).
5. T. T. Chuang, Y. C. Pan, and T. H. Chuang, *J. Alloys & Compounds* **243**, 126 (1996).
6. Y. C. Pan, T. H. Chuang, and Y. D. Yao, *J. Mater. Sci.* **26**, 6097 (1991).
7. W. W. Lee and D. B. Lee, *J. Corros. Sci. Soc. of Kor.* **27**, 603 (1998).
8. I. Barin, *Thermochemical Data of Pure Substances VCH*, Weinhein, Germany (1989).